Available online at www.sciencedirect.com
SCIENCE DIRECT
Journal of Colloid and Interface Science 290 (2005) 1–13
JOURNAL OF Colloid and Interface Science
www.elsevier.com/locate/jcis

Priority communication

Heterogeneous Do–Do model of water adsorption on carbons

Sylwester Furmaniak [a], Piotr A. Gauden [a], Artur P. Terzyk [a,*], Gerhard Rychlicki [a], Radosław P. Wesołowski [a], Piotr Kowalczyk [b]

[a] *Physicochemistry of Carbon Materials Research Group, Department of Chemistry, N. Copernicus University, Gagarin St. 7, 87-100 Toruń, Poland*
[b] *Department III, Institute of Physical Chemistry, Polish Academy of Science, Kasprzaka Street 44/52, 01-224 Warsaw, Poland*

Received 6 June 2005; accepted 20 July 2005

Available online 15 August 2005

Abstract

The model of water adsorption on carbons proposed five years ago by Do and Do is analyzed and improved. Following the experimental evidence that for activated carbons surface active groups differ in the value of the energy of interaction with water molecules, we propose to extend the original model to take this fundamental feature into account. For the original DD model, as well as proposed new heterogeneous one (HDDM), we develop also the corresponding isosteric enthalpy of adsorption formulas. The features of the HDDM are studied via simulations. It is shown that the new model predicts the shapes of adsorption isotherm as well as corresponding enthalpy observed for real experimental systems. Finally, the HDDM is successfully applied to description of arbitrarily chosen adsorption and enthalpy of adsorption data. Up to our knowledge, HDDM is the first model describing satisfactorily water adsorption isotherms and corresponding enthalpy data measured on different microporous activated carbons in the whole relative pressure range.

Keywords: Carbon; Water adsorption; Chemisorption; Microporosity; Hydrophilic centers; Primary adsorption sites; Heat of adsorption; Surface properties

1. Introduction

Although different more or less advanced models of water adsorption have been proposed so far, the theoretical description of water adsorption on carbons is still far from complete [1–12]. Very interesting approach in this field was proposed five years ago by Do and Do who developed the new water adsorption isotherm equation assuming the two-stage mechanism of this process [13]. In this mechanism, at the first stage, water molecules are strongly bonded to the primary adsorption sites and form conglomerates of molecules (via hydrogen bonds). If the number of molecules is equal to six, the conglomerate of five molecules can tear away from the cluster and fill micropores. Thus, the Do–Do model (DD) can be considered as the so-called "hybrid" one in which the first term describes the adsorption on the primary sites (it is of the BET type) and the second term refers to desorption from these sites and the adsorption of the pentamer into the micropores (thus this term describes the micropore filling). Neitsch et al. [14] generalized the DD model assuming that the number of water molecules forming a cluster (i.e., the micropore filling by the m-mers) can be optional. This assumption leads to the final version of the adsorption isotherm equation,

$$a = a_0 \frac{K_f \sum_{n=1}^{N} n h^n}{1 + K_f \sum_{n=1}^{N} h^n} + a_{\mu s} \frac{K_\mu h^m}{1 + K_\mu h^m}, \tag{1}$$

where N is the maximum number of water molecules adsorbed on the surface sites ($N \geqslant m + 1$), a_0 is the concentration of surface active groups, $a_{\mu s}$ is the saturation concentration in the micropore, K_f is the chemisorption and K_μ micropore equilibrium constant, respectively, and h is the relative pressure (equal to p/p_s where p is the equilibrium and p_s the saturation pressure of water, respectively).

It should be pointed out that some simplifications of the DD model were also reported by Zimny and co-workers [15,16], i.e., the first term on the right-hand side of Eq. (1) (BET type equation) was replaced by a so-called Langmuir type function.

* Corresponding author. Fax: +48 056 654 2477.
E-mail address: aterzyk@chem.uni.torun.pl (A.P. Terzyk).

0021-9797/$ – see front matter © 2005 Published by Elsevier Inc.
doi:10.1016/j.jcis.2005.07.043

2. Enthalpy of adsorption from the DD model

Although the DD model seems to satisfy the most of the experimental and theoretical conditions [13–16], it assumes energetic homogeneity of the adsorption sites to simplify the final form of equation. Do and others [13–16] did not derive the enthalpy of adsorption—they limited their studies only to investigation of the properties of the adsorption isotherm equation. Therefore, we decided to expand those considerations. To get an analytical form of adsorption enthalpy equations, i.e., the "pure" isosteric enthalpy of adsorption ($q^{\mathrm{st}} - L$), the well-known thermodynamic van't Hoff equation $q^{\mathrm{st}} - L = RT^2(\partial \ln h/\partial T)_{\mathrm{a}}$ is taken into account. We assume that the maximum adsorption in micropores ($a_{\mu\mathrm{s}}$) depends on the temperature due to the thermal expansion of clusters filling micropores, $a_{\mu\mathrm{s}} = a_{0,\mu\mathrm{s}} \exp[-\alpha(T - T_0)]$. For the temperature dependence of parameters $K_{\mathrm{f}} = K_{0,\mathrm{f}} \exp[q_{\mathrm{f}}/RT]$ and $K_\mu = K_{0,\mu} \exp[q_\mu/RT]$ after differentiation of Eq. (1) with respect to the temperature (and after some simplifications), the following equation describing the isosteric enthalpy of adsorption is obtained,

$$q^{\mathrm{st}} - L = \left[a_0 \frac{K_{\mathrm{f}} \sum_{n=1}^{N} n h^n}{(1 + K_{\mathrm{f}} \sum_{n=1}^{N} h^n)^2} q_{\mathrm{p}} + a_{\mu\mathrm{s}} \frac{K_\mu h^m}{(1 + K_\mu h^m)^2} q_\mu + RT^2 \alpha a_{\mu\mathrm{s}} \frac{K_\mu h^m}{1 + K_\mu h^m} \right] \Bigg/ \left[a_0 \frac{(1 + K_{\mathrm{f}} \sum_{n=1}^{N} h^n) K_{\mathrm{f}} \sum_{n=1}^{N} n^2 h^n - K_{\mathrm{p}}^2 (\sum_{n=1}^{N} n h^n)^2}{(1 + K_{\mathrm{f}} \sum_{n=1}^{N} h^n)^2} + a_{\mu\mathrm{s}} \frac{m K_\mu h^m}{(1 + K_\mu h^m)^2} \right], \tag{2}$$

where R is the gas constant, T is the temperature, and L is the enthalpy of water condensation equal to $RT^2(\mathrm{d} \ln p_{\mathrm{s}}/\mathrm{d}T)$, q_{f} and q_μ are the energies associated with the constants K_{f} and K_μ, and α is the thermal expansion coefficient of water present in the form of clusters in micropores. Pre-exponential factors ($K_{0,\mathrm{f}}$ and $K_{0,\mu}$, respectively) are assumed to be slightly dependent on temperature (so-called entropic factors).

Figs. 1 and 2 show the typical plots of the adsorption isotherms and corresponding isosteric enthalpy of adsorption (Eqs. (1) and (2)). The influence of all parameters of the DD model (i.e., K_{f}, a_0, K_μ, $a_{\mu\mathrm{s}}$, N, or m) is investigated in order to reflect the various surface properties of activated carbon ranging from the very hydrophobic to highly oxidized surfaces. It should be pointed out that the properties of the simpler form of Eq. (1) (i.e., the connection with the mechanism of water adsorption, especially) were recently investigated by Do and Do [13] (their studies were limited only to the simulation of adsorption isotherms). Therefore, we take into account the same or similar values of parameters as used in [13]. From the analysis of the plots generated on the basis of various sets of parameters, Do and Do [13] concluded that water adsorption isotherm curves can be basically divided into three distinct regions. The first region (where the reduced pressure is less than 0.2) represents the adsorption around the functional groups, where the mechanism is simply chemisorption and hydrogen bonding. The second region is between 0.3 and 0.8, where water concentration around the functional groups is high enough to induce the adsorption into the micropore. The third region is when the reduced pressure is greater than 0.8, and this is the region where the cluster is filling up the free space of pores.

From the analysis of the plots collected in Figs. 1 and 2 it is seen that an increase in five variables (m is the exception) causes an increase in the amount adsorbed at various ranges of the reduced pressure. From the point of view of the thermodynamic verification of the analyzed theoretical model, the first region (where the reduced pressure is about less than 0.2) is the most important one. It can be observed that insignificant differences exist between the plots of ($q^{\mathrm{st}} - L$) for the fixed values of K_μ, $a_{\mu\mathrm{s}}$, N, and m. On the other hand, both parameters of the first term of Eq. (1) have a significant influence on ($q^{\mathrm{st}} - L$). One can see that an increase in K_{f} and/or a_0 causes a faster and different increase in the amount adsorbed and such an increase occurs at lower reduced pressures. On the other hand, for higher values of adsorption the influence of the thermal expansion parameter of water on the "pure" isosteric enthalpy is a dominating factor for the all plots. The main feature of the DD model is that the plots of the isosteric enthalpy of adsorption shown in Figs. 1 and 2 are usually decreasing with adsorbed amount. In fact, this type of plots has been observed recently for some experimental data determined for a series of microporous activated carbons, usually for the unmodified chemically adsorbents [3,4,6,7,9,10,17–20] and also in some theoretical studies [4,6–10]. It should be mentioned here that also different kind (i.e., the increasing one) of the plot of adsorption enthalpy can be easily generated from the original DD model.

3. Developing the heterogeneous DD model (HDDM)

In this part, based on the original DD approach [13], we present the derivation of new adsorption isotherm equation. Although the fundamentals of this development are similar to the original proposed by Do and Do, it is remarkably modified by us. The major assumptions are based on the well-known experimental fact that surface active groups of carbons are of different kinds. It is well known that the typical surface groups of carbons can be divided, based, for example, on the $\mathrm{p}K_{\mathrm{a}}$ values, and that is why it is impossible for them to adsorb water with the same adsorption energy [1–4,21–23].

Thus, assuming that a few types of surface primary adsorption sites (P^i) are present on carbon surface, and due to strong adsorption (chemisorption) each center can attach one molecule of water (A), we can write

$$P^i + A \leftrightarrow P^i A \ (\equiv S^i). \tag{3}$$

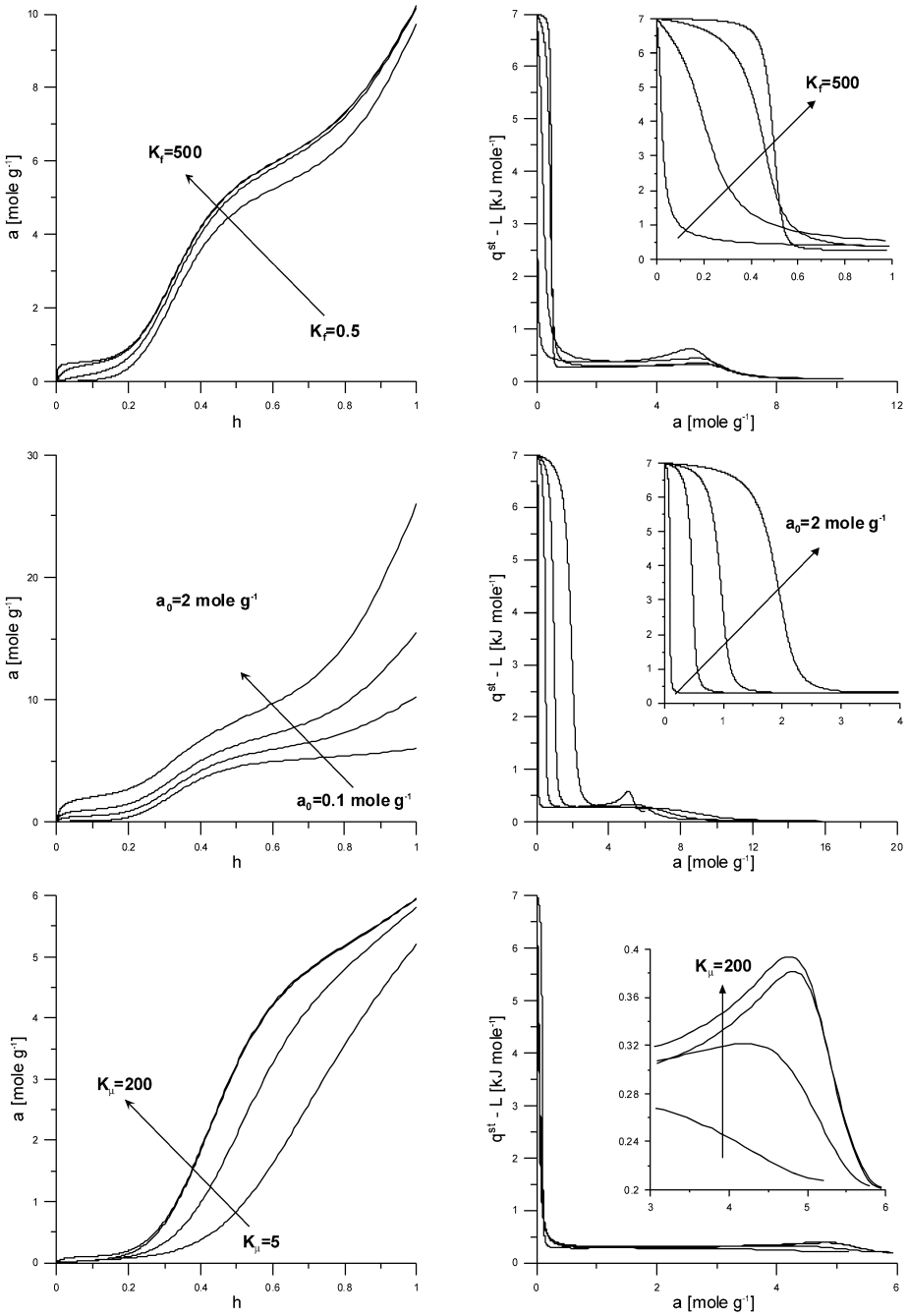

Fig. 1. The DD model—the effect of the chemisorption equilibrium constant, K_f ($a_0 = 0.5\,\mathrm{mol\,g^{-1}}$, $K_\mu = 200$, $a_{\mu\mathrm{s}} = 5\,\mathrm{mol\,g^{-1}}$, $m = 5$, and $N = 20$), the surface sites concentration, a_0 ($K_\mathrm{f} = 100$, $K_\mu = 200$, $a_{\mu\mathrm{s}} = 5\,\mathrm{mol\,g^{-1}}$, $m = 5$, and $N = 20$), and the micropore equilibrium constant, K_μ ($K_\mathrm{f} = 5$, $a_0 = 0.1\,\mathrm{mol\,g^{-1}}$, $a_{\mu\mathrm{s}} = 5\,\mathrm{mol\,g^{-1}}$, $m = 5$, and $N = 20$) on the shape of the isotherm and the corresponding isosteric adsorption enthalpy (Eqs. (1) and (2), respectively) for $q_\mathrm{f} = 7\,\mathrm{kJ\,mol^{-1}}$, $q_\mu = 1.25\,\mathrm{kJ\,mol^{-1}}$, $\alpha = 1.8 \times 10^{-4}\,\mathrm{K^{-1}}$, $L = 43.96\,\mathrm{kJ\,mol^{-1}}$, and $T = 298\,\mathrm{K}$.

Each adsorbed molecule transforms into secondary adsorption site (S^i), where subsequent water molecules are attached via hydrogen bonds. On species adsorbed in that way the next water molecules are adsorbed in the same way:

$$S^i + A \leftrightarrow S^i A,$$
$$S^i A + A \leftrightarrow S^i A_2,$$
$$\vdots$$
$$S^i A_{n-1} + A \leftrightarrow S^i A_n. \tag{4}$$

We postulate that due to strong adsorption of primary water molecules, this process is independent of the bonding of the next molecules, i.e., contrary to Do and Do [13] we postulate that the bonding of the next water molecules does not influence the equilibrium of the process described by Eq. (3). That is the reason why adsorption on primary sites can be described by the Langmuir adsorption isotherm equation.

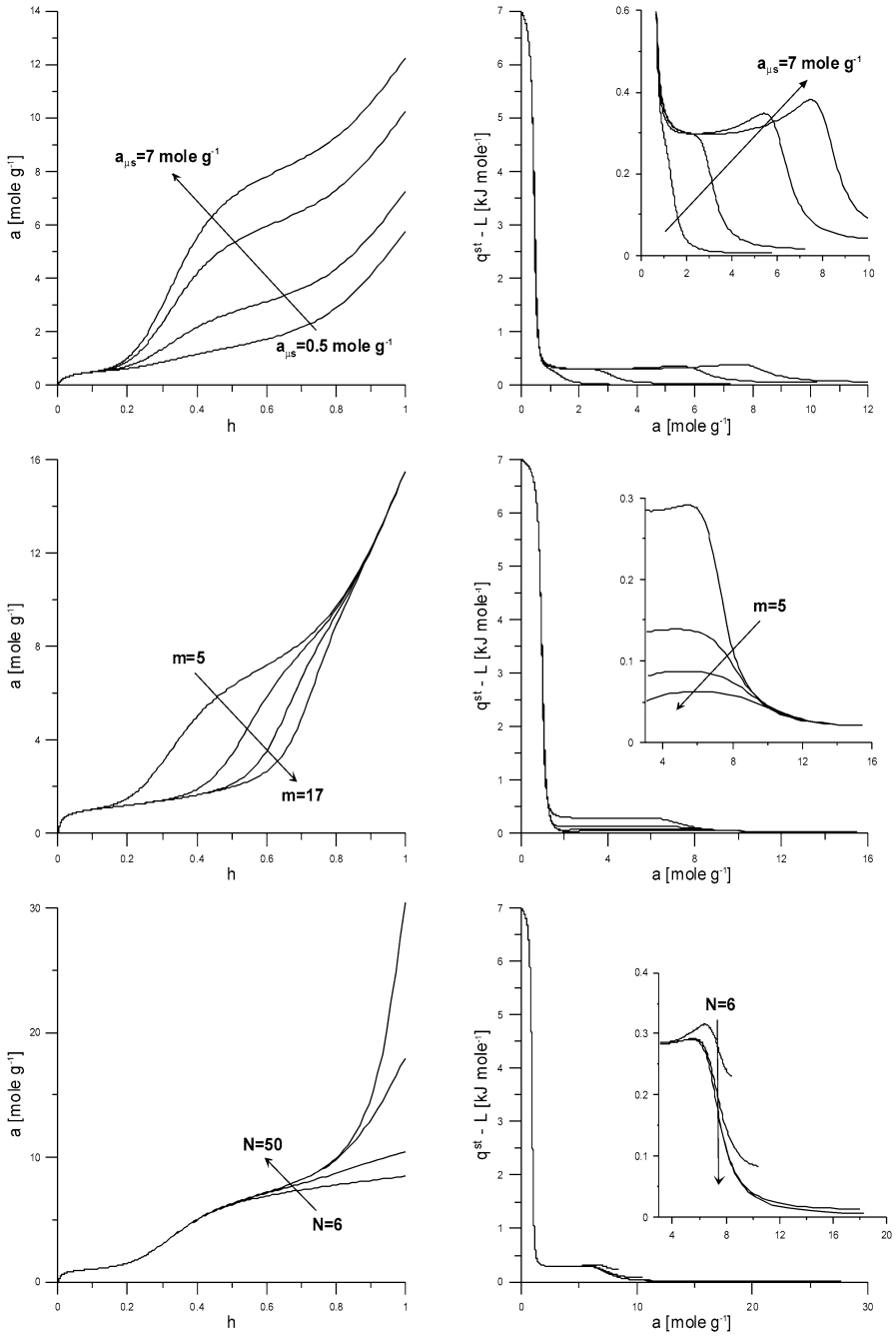

Fig. 2. The DD model—the effect of the saturation concentration in the micropore, $a_{\mu s}$ ($K_f = 50$, $a_0 = 0.5\ \mathrm{mol\,g^{-1}}$, $K_\mu = 200$, $m = 5$, and $N = 20$), the number of adsorbed water molecules in micropore per cluster, m ($K_f = 100$, $a_0 = 1\ \mathrm{mol\,g^{-1}}$, $K_\mu = 200$, $a_{\mu s} = 5\ \mathrm{mol\,g^{-1}}$, and $N = 20$), and the number of adsorbed water molecules on the surface group, N ($K_f = 100$, $a_0 = 1\ \mathrm{mol\,g^{-1}}$, $K_\mu = 200$, $a_{\mu s} = 5\ \mathrm{mol\,g^{-1}}$, and $m = 5$) on the shape of the isotherm and the corresponding isosteric adsorption enthalpy (Eqs. (1) and (2), respectively).

The total adsorption on primary sites (a_{prim}) is given by the sum,

$$a_{\mathrm{prim}} = \sum_i a_{\mathrm{prim},i} = \sum_i \frac{a_{\mathrm{mL},i} K_{\mathrm{L},i} h}{1/p_s + K_{\mathrm{L},i} h}, \tag{5}$$

where $a_{\mathrm{prim},i}$ is the adsorption on ith kind of adsorption center and $a_{\mathrm{mL},i}$ is the surface concentration of ith center, while $K_{\mathrm{L},i}$ is the Langmuir constant.

Following Do and Do [13] we postulate that the constants of reactions (4) are the same (K_p^*) due to hydrogen bonding mechanism. Those constants are given by

$$\frac{[S^i A]}{[S^i][A]} = K_p^* = \frac{[S^i A_n]}{[S^i A_{n-1}][A]}, \tag{6}$$

where the brackets denote the concentrations of the respective reagents. Since the equilibrium concentration of the adsorbate ($[A]$) is linearly dependent on the pressure, Eq. (6)

can be rewritten in the following form:

$$\frac{[S^i A]}{[S^i]h} = K_\mathrm{p} = \frac{[S^i A_n]}{[S^i A_{n-1}]h}. \tag{7}$$

After simple manipulation we obtain

$$[S^i A] = K_\mathrm{p}[S^i]h \quad \text{and}$$
$$[S^i A_n] = K_\mathrm{p}[S^i A_{n-1}]h = K_\mathrm{p}^n[S^i]h^n. \tag{8}$$

At the equilibrium,

$$\sum_i [S^i] + \sum_i [S^i A] + \sum_i [S^i A_2] + \cdots + \sum_i [S^i A_n] + \cdots = a_\mathrm{prim}. \tag{9}$$

Equations (8) and (9) can be transformed into the following form:

$$\sum_i [S^i] + \sum_i K_\mathrm{p}[S^i]h + \sum_i K_\mathrm{p}^2[S^i]h^2 + \cdots + \sum_i K_\mathrm{p}^n[S^i]h^n + \cdots = \sum_i [S^i]\left(1 + \sum_{n=1} K_\mathrm{p}^n h^n\right) = a_\mathrm{prim}. \tag{10}$$

The value of adsorption on secondary centers is equal to

$$a_\mathrm{sec} = \sum_i [S^i A] + \sum_i 2[S^i A_2] + \cdots + \sum_i n[S^i A_n] + \cdots. \tag{11}$$

From Eqs. (8) and (11) one obtains

$$a_\mathrm{sec} = \sum_i K_\mathrm{p}[S^i]h + \sum_i 2K_\mathrm{p}^2[S^i]h^2 + \cdots + \sum_i nK_\mathrm{p}^n[S^i]h^n + \cdots = \sum_i [S^i] \sum_{n=1} nK_\mathrm{p}^n h^n. \tag{12}$$

Taking into account Eq. (10) we obtain the final equation describing adsorption on secondary centers:

$$a_\mathrm{sec} = \frac{a_\mathrm{prim} \sum_{n=1} nK_\mathrm{p}^n h^n}{1 + \sum_{n=1} K_\mathrm{p}^n h^n} = \sum_i \frac{a_{\mathrm{mL},i} K_{\mathrm{L},i} h}{1/p_\mathrm{s} + K_{\mathrm{L},i} h} \frac{\sum_{n=1} nK_\mathrm{p}^n h^n}{1 + \sum_{n=1} K_\mathrm{p}^n h^n}. \tag{13}$$

Following Do and Do [13] we assume that micropores are filled via clusters, created from conglomerates of water molecules attached to secondary adsorption sites. Similarly to Neitsch et al. [14] we assume that those clusters contain m molecules each, i.e., $S^i A_n \leftrightarrow [A_m]_\mu + S^i A_{n-m}$ for $n \geqslant m$.

The respective equations describing the rate of adsorption and desorption of those clusters are given by

$$r_\mathrm{a} = k_{\mu\mathrm{a}}(V_\mu - V_{A_m}) \sum_i \sum_{n=m} [S^i A_n], \tag{14}$$

$$r_\mathrm{d} = k_{\mu\mathrm{d}} V_{A_m} \sum_i \sum_{n=m} [S^i A_{n-m}], \tag{15}$$

where V_μ is the total micropore volume and V_{A_m} is the volume of pores occupied by clusters.

From Eqs. (14) and (15) we obtain

$$V_{A_m} = V_\mu \frac{K_\mu \sum_i \sum_{n=m} [S^i A_n]}{K_\mu \sum_i \sum_{n=m} [S^i A_n] + \sum_i \sum_{n=m} [S^i A_{n-m}]}, \tag{16}$$

where $K_\mu = k_{\mu\mathrm{a}}/k_{\mu\mathrm{d}}$.

Dividing Eq. (16) by the molar volume of clusters we obtain the equation describing adsorption connected with clusters filling micropores (a_μ),

$$a_\mu = a_{\mu\mathrm{s}} \frac{K_\mu \sum_i \sum_{n=m} [S^i A_n]}{K_\mu \sum_i \sum_{n=m} [S^i A_n] + \sum_i \sum_{n=m} [S^i A_{n-m}]}, \tag{17}$$

where $a_{\mu\mathrm{s}}$ is the maximum adsorption in micropores limited by the micropore volume.

From Eqs. (8) and (17) one obtains

$$a_\mu = a_{\mu\mathrm{s}} K_\mu \sum_i \sum_{n=m} K_\mathrm{p}^n [S^i] h^n \Bigg/ \left[K_\mu \sum_i \sum_{n=m} K_\mathrm{p}^n [S^i] h^n + \sum_i \sum_{n=m} K_\mathrm{p}^{n-m} [S^i] h^{n-m} \right]. \tag{18}$$

Equation (18) can be written in the simplified form as

$$a_\mu = \frac{a_{\mu\mathrm{s}} K_\mu K_\mathrm{p}^m h^m}{1 + K_\mu K_\mathrm{p}^m h^m}. \tag{19}$$

Since $K = K_\mu K_\mathrm{p}^m$, the final version of the equation describing adsorption in micropores can be written as

$$a_\mu = \frac{a_{\mu\mathrm{s}} K h^m}{1 + K h^m}. \tag{20}$$

Thus, the total adsorption of water is equal to

$$a = a_\mathrm{prim} + a_\mathrm{sec} + a_\mu, \tag{21}$$

$$a = \sum_i \frac{a_{\mathrm{mL},i} K_{\mathrm{L},i} h}{1/p_\mathrm{s} + K_{\mathrm{L},i} h} \left(1 + \frac{\sum_{n=1}^N nK_\mathrm{p}^n h^n}{1 + \sum_{n=1}^N K_\mathrm{p}^n h^n}\right) + a_{\mu\mathrm{s}} \frac{K h^m}{1 + K h^m} = a_\mathrm{prim} \left(1 + \frac{\sum_{n=1}^N nK_\mathrm{p}^n h^n}{1 + \sum_{n=1}^N K_\mathrm{p}^n h^n}\right) + a_{\mu\mathrm{s}} \frac{K h^m}{1 + K h^m}, \tag{22}$$

where N should be treated as the best-fit parameter.

4. The development of the isosteric enthalpy of adsorption equation

To develop the equation describing the isosteric enthalpy of adsorption, corresponding to Eq. (22), we assumed the following forms of constants, $K_{\mathrm{L},i} = K_{\mathrm{L},0,i} \exp[q_{\mathrm{L},i}/RT]$,

$K_p = K_p \exp[q_p/RT]$, and $K = K_0 \exp[q/RT]$, where pre-exponential factors are again assumed to be slightly dependent on temperature entropic factors, and q_x are the values of enthalpy connected with the respective constants. After differentiation of both sides of Eq. (22) and after simple manipulation one obtains

$$q^{st} - L = \left[\left(\sum_i \frac{a_{mL,i}\, p_s K_{L,i} h}{(1 + p_s K_{L,i} h)^2}(q_{L,i} - L)\right)\left(1 + \frac{\Theta_n}{1+\Theta}\right) + a_{prim}\frac{(1+\Theta)\Theta_{n2} - \Theta_n^2}{(1+\Theta)^2} q_p + \frac{a_{\mu s} K h^m}{(1+Kh^m)^2} q + RT^2 \alpha a_{\mu s} \frac{Kh^m}{1+Kh^m}\right] \Bigg/ \left[\left(\sum_i \frac{a_{mL,i}\, p_s K_{L,i} h}{(1 + p_s K_{L,i} h)^2}\right)\left(1 + \frac{\Theta_n}{1+\Theta}\right) + a_{prim}\frac{(1+\Theta)\Theta_{n2} - \Theta_n^2}{(1+\Theta)^2} + \frac{m a_{\mu s} K h^m}{(1+Kh^m)^2}\right], \quad (23)$$

where $\Theta = \sum_{n=1}^{N} K_p^n h^n$, $\Theta_n = \sum_{n=1}^{N} n K_p^n h^n$, $\Theta_{n2} = \sum_{n=1}^{N} n^2 K_p^n h^n$, and a_{prim} is given by Eq. (5).

Due to differences in constants, the direct comparison of the original Do–Do model (Eqs. (1) and (2)) with the heterogeneous one (Eqs. (22) and (23)) is impossible. The major reason is the assumption made in the original model that $h = K_p[A]$. On the other hand, in Fig. 3 the typical contribution of all types of adsorption into global adsorption value (for arbitrarily chosen parameters) is shown in order to explain the properties of Eq. (22). From this figure it is seen that water adsorption isotherm curves can be again divided into three different regions. Then, the same conclusions as from the analysis of plots (Figs. 1 and 2) generated on the basis of the homogeneous DD model (Eq. (1)) can be drawn. However, the new adsorption equation developed in this study made it possible to obtain different interesting shapes of $(q^{st} - L)$ (impossible to generate from the original DD model).

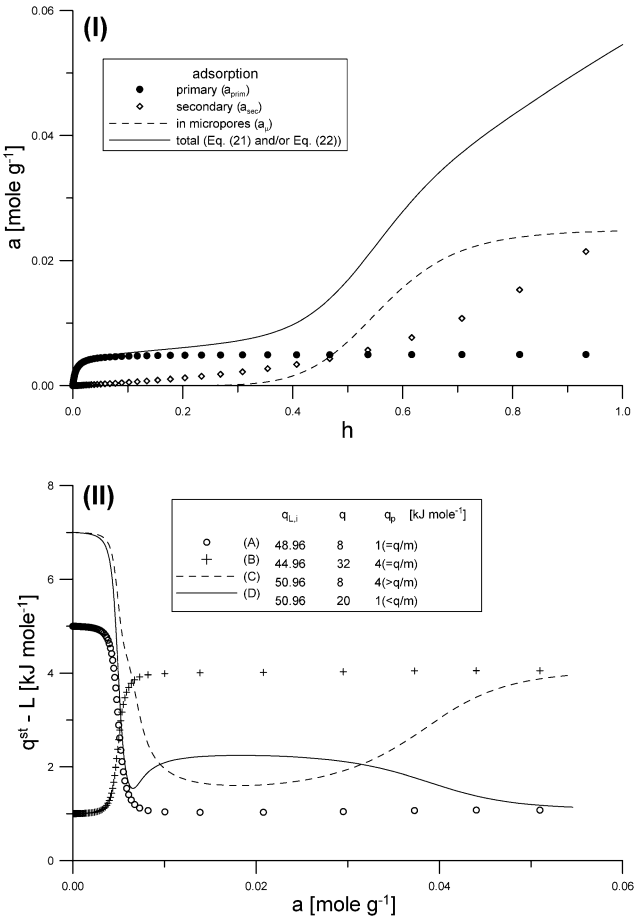

Fig. 3. (I) The contribution of different types of adsorption (a_{prim}, a_{sec} and a_μ) to total adsorption described by Eq. (22). (II) The influence of the relations between q_L, q_p and q on the plot of the isosteric enthalpy of adsorption calculated from Eq. (23) for $a_{mL} = 0.005$ mol g^{-1}, $K_L = 0.05$ Pa^{-1}, $K_p = 1$, $a_{\mu s} = 0.025$ mol g^{-1}, $K = 100$, $m = 8$, $N = 10$, $p_s = 3167.2$ Pa, $\alpha = 1.8 \times 10^{-4}$ K^{-1}, $L = 43.96$ kJ mol^{-1}, and $T = 298$ K.

5. Simulation of the main features of the new model

Since the adsorption enthalpy values related to the considered types of adsorption processes (Eq. (21): $a_{prim,i}$, a_{sec} and a_μ) are assumed to be constant ($q_{L,i}$, q_p and q/m, respectively), the value of the total adsorption enthalpy (Eq. (23)) can be considered as the weighing average of the enthalpy connected with the mentioned types of adsorption [24] (Fig. 3). The weight is here the contribution of the rise in adsorption (according to the considered model) to the total adsorption value. Considering the plots of the adsorption isotherms (Fig. 3) and the contribution of the components into the adsorption value, one can conclude that at low pressures mainly the interactions between water molecules and the primary adsorption centers are responsible for the values of the adsorption enthalpy. The secondary adsorption (i.e., the creation of conglomerates of water molecules) increases in the whole pressure range, and it contributes remarkably after the primary sites are filled (and at higher pressures). This effect is clearly visible on the curve D (Fig. 3(II)) where one can observe minima at adsorption ca. 0.07 mol g^{-1} and the decreasing plot of adsorption enthalpy for larger loadings. In the range of intermediate relative pressures the pore filling process by water clusters (a_μ) is mainly responsible for the rise in adsorption.

In Fig. 4 we assumed the existence of three types of primary adsorption sites characterized by different energy of interaction with water molecules. The magnitudes of K_L influence the rate of saturation of the respective centers (the centers adsorbing with the larger value of Langmuir constant are labeled as “first,” those adsorbing with intermediate value are labeled as “second” and finally, those with the smallest K_L value are labeled as “third”). The differences in the rates of saturation of the primary centers are responsible

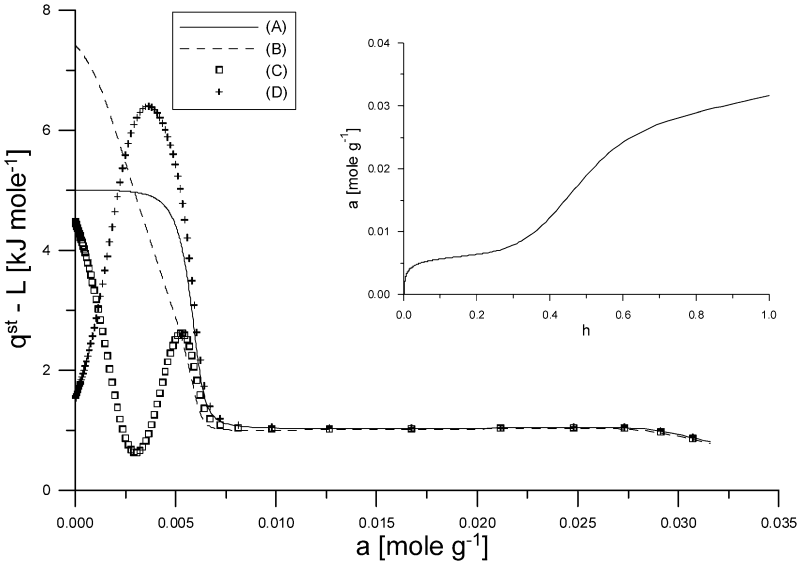

Fig. 4. The plots of the adsorption enthalpy generated from Eq. (23) assuming three different types of surface primary adsorption sites: $a_{\mathrm{mL},1} = a_{\mathrm{mL},2} = a_{\mathrm{mL},3} = 0.002\ \mathrm{mol\,g^{-1}}$; $K_{\mathrm{L},1} = 0.3\ \mathrm{Pa^{-1}}$; $K_{\mathrm{L},2} = 0.05\ \mathrm{Pa^{-1}}$; $K_{\mathrm{L},3} = 0.01\ \mathrm{Pa^{-1}}$; $K_{\mathrm{p}} = 0.5$; $a_{\mu\mathrm{s}} = 0.02\ \mathrm{mol\,g^{-1}}$; $K = 80$; $m = 6$; $N = 10$; $q_{\mathrm{p}} = 0.5\ \mathrm{kJ\,mol^{-1}}$; $q = 6\ \mathrm{kJ\,mol^{-1}}$. (A) $q_{\mathrm{L},1} = q_{\mathrm{L},2} = q_{\mathrm{L},3} = 48.96\ \mathrm{kJ\,mol^{-1}}$; (B) $q_{\mathrm{L},1} = 51.96\ \mathrm{kJ\,mol^{-1}}$; $q_{\mathrm{L},2} = 48.96\ \mathrm{kJ\,mol^{-1}}$; $q_{\mathrm{L},3} = 45.96\ \mathrm{kJ\,mol^{-1}}$; (C) $q_{\mathrm{L},1} = 49.96\ \mathrm{kJ\,mol^{-1}}$; $q_{\mathrm{L},2} = 38.96\ \mathrm{kJ\,mol^{-1}}$; $q_{\mathrm{L},3} = 49.96\ \mathrm{kJ\,mol^{-1}}$; (D) $q_{\mathrm{L},1} = 43.96\ \mathrm{kJ\,mol^{-1}}$; $q_{\mathrm{L},2} = 53.96\ \mathrm{kJ\,mol^{-1}}$; $q_{\mathrm{L},3} = 48.96\ \mathrm{kJ\,mol^{-1}}$.

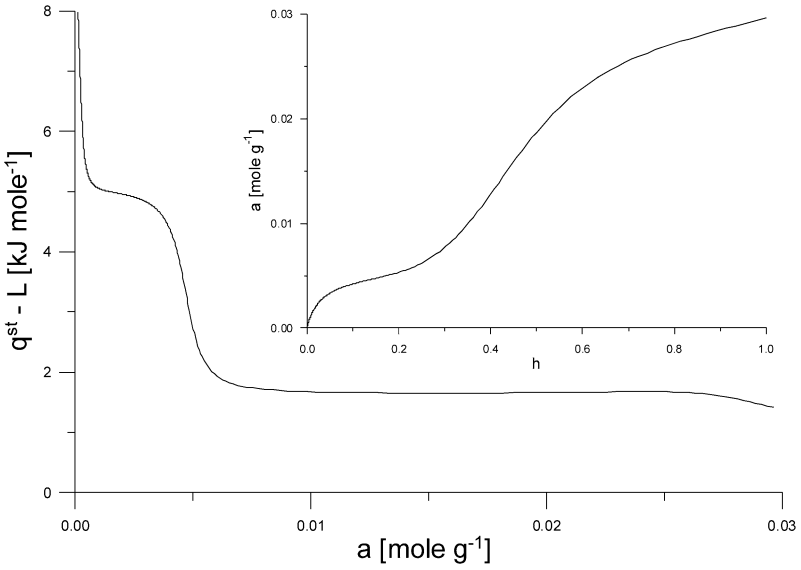

Fig. 5. The stepwise enthalpy plot generated from Eq. (23): $a_{\mathrm{mL},1} = 0.0002\ \mathrm{mol\,g^{-1}}$; $a_{\mathrm{mL},2} = 0.005\ \mathrm{mol\,g^{-1}}$; $K_{\mathrm{L},1} = 1\ \mathrm{Pa^{-1}}$; $K_{\mathrm{L},2} = 0.01\ \mathrm{Pa^{-1}}$; $K_{\mathrm{p}} = 0.5$; $a_{\mu\mathrm{s}} = 0.02\ \mathrm{mol\,g^{-1}}$; $K = 50$; $m = 5$; $N = 10$; $q_{\mathrm{L},1} = 53.96\ \mathrm{kJ\,mol^{-1}}$; $q_{\mathrm{L},2} = 48.96\ \mathrm{kJ\,mol^{-1}}$; $q_{\mathrm{p}} = 1\ \mathrm{kJ\,mol^{-1}}$; $q = 8\ \mathrm{kJ\,mol^{-1}}$.

for the plots of the enthalpy in the initial range of adsorption. Initially the energy of interactions between water molecules and the "first" adsorption sites dominate, and the influence of interactions with "second" and "third" sites is visible at larger adsorptions. If we assume that the energy of interaction is the same for all three types of sites (curve A), one can observe the appearance of the plateau on the enthalpy plot. On the contrary, if the energies decrease in the same sequence as the values of K_{L} (curve B) the decreasing plot of the enthalpy (in the range of interactions with adsorption centers) is observed. The assumption that the energy of interaction of water molecules with second sites is lower (or larger) than with first and third sites (curves C and D) leads to the non-monotonically plots of the adsorption enthalpy.

The assumption of the existence of two types of adsorption centers (Fig. 5), i.e., present in smaller amount but adsorbing with larger K_{L} value (and having larger energy of interaction with water molecules), and present in larger amount but having smaller K_{L} value (and interacting with smaller adsorption energy), leads to the stepwise plot of the adsorption enthalpy. It can be noticed, that the width of the step is strictly related to the concentration of the second sites.

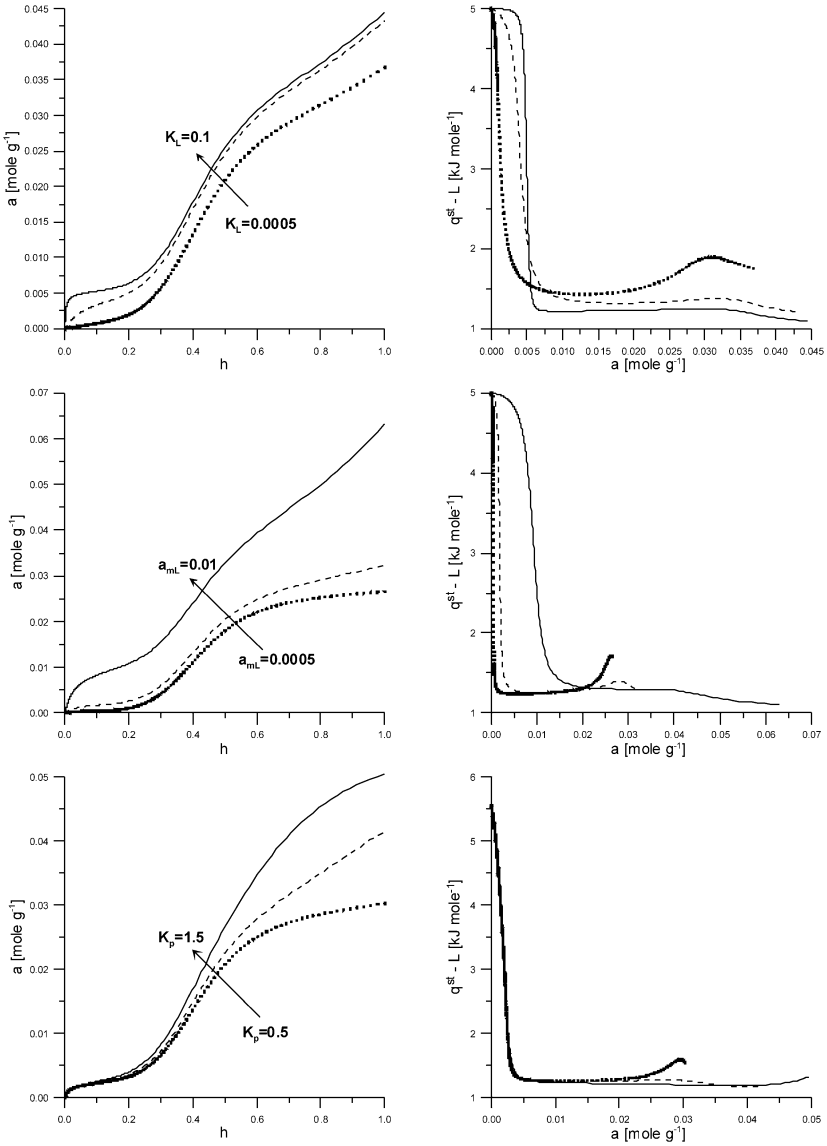

Fig. 6. The heterogeneous Do–Do model—the influence of the Langmuir constant K_{L} (the existence of only one type of adsorption sites was assumed; $a_{\mathrm{mL}} = 0.005\ \mathrm{mol\,g^{-1}}$; $K_{\mathrm{p}} = 0.8$; $a_{\mu\mathrm{s}} = 0.025\ \mathrm{mol\,g^{-1}}$; $K = 70$; $m = 5$; $N = 10$), the concentration of primary adsorption sites a_{mL} (the existence of only one type of the adsorption sites was assumed; $K_{\mathrm{L}} = 0.01\ \mathrm{Pa^{-1}}$; $K_{\mathrm{p}} = 0.8$; $a_{\mu\mathrm{s}} = 0.025\ \mathrm{mol\,g^{-1}}$; $K = 70$; $m = 5$; $N = 10$), and the constant K_{p} ($a_{\mathrm{mL},1} = a_{\mathrm{mL},2} = a_{\mathrm{mL},3} = 0.001\ \mathrm{mol\,g^{-1}}$; $K_{\mathrm{L},1} = 0.05\ \mathrm{Pa^{-1}}$; $K_{\mathrm{L},2} = 0.01\ \mathrm{Pa^{-1}}$; $K_{\mathrm{L},3} = 0.002\ \mathrm{Pa^{-1}}$; $a_{\mu\mathrm{s}} = 0.025\ \mathrm{mol\,g^{-1}}$; $K = 70$; $m = 5$; $N = 10$) on the shape of the isotherm and the corresponding isosteric adsorption enthalpy (Eqs. (22) and (23), respectively) for $q_{\mathrm{L}} = 48.96\ \mathrm{kJ\,mol^{-1}}$, $q_{\mathrm{p}} = 1\ \mathrm{kJ\,mol^{-1}}$, $q = 6\ \mathrm{kJ\,mol^{-1}}$, $\alpha = 1.8 \times 10^{-4}\ \mathrm{K^{-1}}$, $L = 43.96\ \mathrm{kJ\,mol^{-1}}$, and $T = 298$ K.

The change in the shape of the adsorption isotherm from type IV to type V with the decrease in K_{L} value (Fig. 6) is connected with the change of the quantitative character of adsorption on primary sites from Langmuir to Henry's type. On related adsorption enthalpy plot one can observe the shrinkage of the initial region (related to the interactions with active centers) and vanishing of the contribution to the global adsorption of adsorption on active centers. Lower and not complete filling of the primary centers leads to the decrease in secondary adsorption (a_{sec}) and, as a consequence, on the enthalpy plots at larger adsorptions the characteristic maxima appear (caused by taking into account the temperature dependence of the maximum adsorption in micropores). The decrease in concentration of the primary adsorption centers (a_{mL}, Fig. 6) has the same influence on the enthalpy plots as (discussed above) changes in the K_{L} values. The rise in K_{p} (Fig. 6) leads to the rise in adsorption on secondary centers, and vanishing of the maximum at larger adsorption values. The rise in $a_{\mu\mathrm{s}}$ (Fig. 7) leads to the rise in adsorption in micropores (a_{μ}). This causes the lengthening of the middle region on the enthalpy plot since adsorption in micropores is responsible for this region. The rise in K (Fig. 7) leads to the rise in adsorption in micropores observed at intermediate pressures. Also the maximum on the enthalpy plot (caused by taking into account the temperature dependence of the maximum adsorption in micropores)

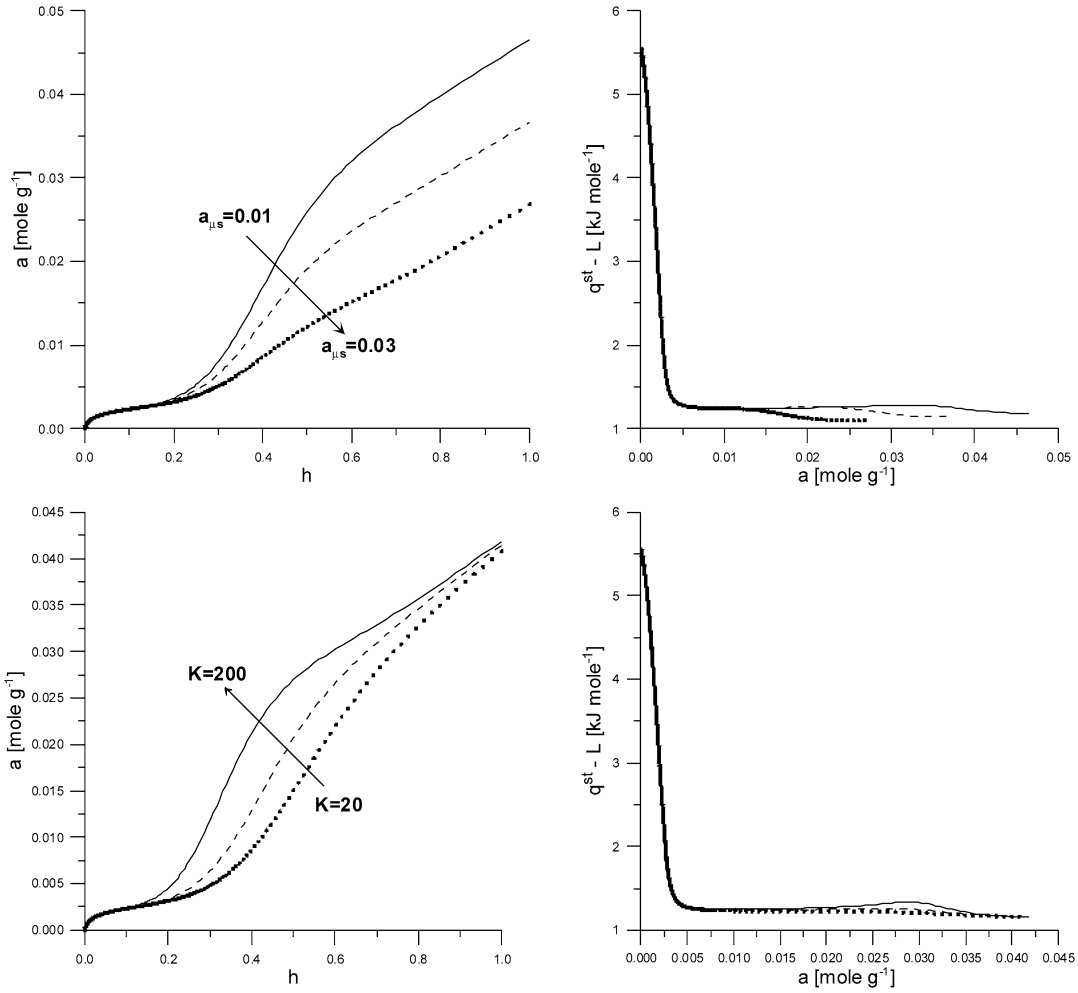

Fig. 7. The heterogeneous Do–Do model—the influence of the maximum adsorption in micropores $a_{\mu s}$ ($a_{\mathrm{mL},1} = a_{\mathrm{mL},2} = a_{\mathrm{mL},3} = 0.001\ \mathrm{mol\,g^{-1}}$; $K_{\mathrm{L},1} = 0.05\ \mathrm{Pa^{-1}}$; $K_{\mathrm{L},2} = 0.01\ \mathrm{Pa^{-1}}$; $K_{\mathrm{L},3} = 0.002\ \mathrm{Pa^{-1}}$; $K_{\mathrm{p}} = 1$; $K = 70$; $m = 5$; $N = 10$) and the constant K ($a_{\mathrm{mL},1} = a_{\mathrm{mL},2} = a_{\mathrm{mL},3} = 0.001\ \mathrm{mol\,g^{-1}}$; $K_{\mathrm{L},1} = 0.05\ \mathrm{Pa^{-1}}$; $K_{\mathrm{L},2} = 0.01\ \mathrm{Pa^{-1}}$; $K_{\mathrm{L},3} = 0.002\ \mathrm{Pa^{-1}}$; $K_{\mathrm{p}} = 1$; $a_{\mu s} = 0.025\ \mathrm{mol\,g^{-1}}$; $m = 5$; $N = 10$) on the shape of the isotherm and the corresponding isosteric adsorption enthalpy (Eqs. (22) and (23), respectively).

is distinct. The decrease in the value of m (Fig. 8) causes the shifting of the jump on isotherms up to larger pressures. The corresponding decrease in adsorption enthalpy is observed at intermediate adsorptions where adsorption in micropores dominates. The influence of N (Fig. 8) on adsorption isotherms is visible only at high pressures. The value of this parameter has practically no influence on the adsorption enthalpy plot.

Summing up, the most important feature of the HDDM is the possibility to predict the steps on the adsorption enthalpy curves.

6. The description of experimental data

Equations (1) with (2) and (22) with (23) were verified for three water-activated carbon systems described previously [4,7,19,20]. Polymeric carbons obtained from polyfurfuryl alcohol were used as adsorbents. Pure furfuryl alcohol was distilled twice, and the polymer was obtained after adding HCl. The polyfurfuryl alcohol obtained was carbonized in a vacuum. The initial adsorbent (carbon A) was prepared by the activation of the obtained in such a way adsorbent with carbon dioxide, and it was followed by annealing in a flow of hydrogen. It should be pointed out here that such a procedure led to a negligibly small concentration of oxygen groups being present on the surface of carbon A. Carbon B was obtained by the oxidation of carbon A for 2 h with concentrated nitric acid. Carbon D was obtained via ionic exchange process by the immersion of carbon B for 7 days in the solution of Na(OH). The details of the procedure of determination of metal contents as well as some additional details concerning the preparation of carbons were given previously [4,7,19,20]. We have chosen the data of water adsorption ($T = 298$ K) on those three samples since they represent different shapes of adsorption isotherms, and (what is more important) different plots of the related differential enthalpy data (measured calorimetrically). Thus, for carbon A monotonically decreasing enthalpy is observed, while for the

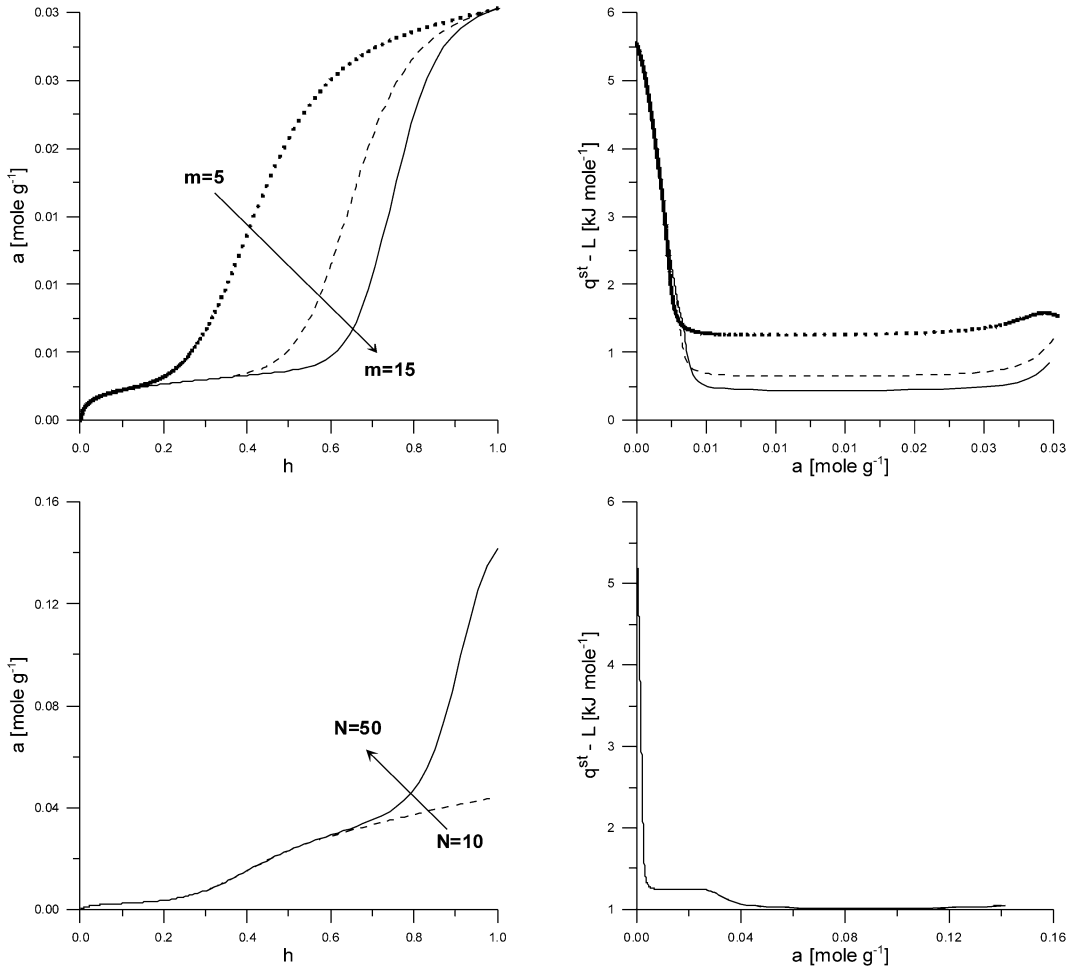

Fig. 8. The heterogeneous Do–Do model—the influence of the parameter m ($a_{\mathrm{mL},1} = a_{\mathrm{mL},2} = a_{\mathrm{mL},3} = 0.001\ \mathrm{mol\,g^{-1}}$; $K_{\mathrm{L},1} = 0.05\ \mathrm{Pa^{-1}}$; $K_{\mathrm{L},2} = 0.01\ \mathrm{Pa^{-1}}$; $K_{\mathrm{L},3} = 0.002\ \mathrm{Pa^{-1}}$; $K_{\mathrm{p}} = 0.5$; $a_{\mu\mathrm{s}} = 0.025\ \mathrm{mol\,g^{-1}}$; $K = 70$; $N = 20$) and the constant K ($a_{\mathrm{mL},1} = a_{\mathrm{mL},2} = a_{\mathrm{mL},3} = 0.001\ \mathrm{mol\,g^{-1}}$; $K_{\mathrm{L},1} = 0.05\ \mathrm{Pa^{-1}}$; $K_{\mathrm{L},2} = 0.01\ \mathrm{Pa^{-1}}$; $K_{\mathrm{L},3} = 0.002\ \mathrm{Pa^{-1}}$; $K_{\mathrm{p}} = 1.1$; $a_{\mu\mathrm{s}} = 0.025\ \mathrm{mol\,g^{-1}}$; $K = 70$; $m = 5$) on the shape of the isotherm and the corresponding isosteric adsorption enthalpy (Eqs. (22) and (23), respectively).

two remaining adsorbents more or less pronounced steps on $(q^{\mathrm{st}} - L)$ curves occur.

The adsorption isotherm and related enthalpy relationships are fitted to experimental data by applying the minimization procedure using the differential evolution (DE) algorithm proposed by Storn and Price [25,26]. DE is a very simple heuristic approach for minimizing non-linear and non-differentiable continuous space functions. Moreover, we recently used successfully this algorithm [9,27]. To optimize objective function (ofunc: $[1 - \{(1 - \mathrm{DC_{iz}})(1 - \mathrm{DC_{qst}})\}^{0.5}]$, where DC are the determination coefficients) with DE, the following settings for the input file are taken into account: DE/best/2/bin method is chosen (this time, the new vector to be perturbed is the best performing vector of the current generation); the number of parents (i.e., number of population members) NP is 10 times greater than the number of parameters of the objective function, D; weighting factor F is equal to 0.8 and crossover probability constant $\mathrm{CR} = 0.5$; the value to reach VTR is equal to 10^{-15} (the procedure stops when ofunc $<$ VTR, if either the maximum number of iterations (generations) itermax is reached, or the best parameter vector bestmem has found a value $f(\mathrm{bestmem}) \leqslant \mathrm{VTR}$). The algorithm seems to work well only if $[\mathrm{XV_{min}}, \mathrm{XV_{max}}]$ covers the region where the global minimum is expected. Therefore, we have taken into account the very wide ranges of XV. Moreover, the calculations are repeated at least five times.

In the case of Eqs. (22) and (23) the objective function is given in the form ofunc: $[1 - \mathrm{DC_{qst}}]$ due to time-consuming calculations. However, we limited a priori the minimum value of $\mathrm{DC_{iz}}$ (> 0.985). Additionally, we limited the values of adsorption tending to the highest values of relative pressure: $\mathrm{ads_{max,teor}} \in (\mathrm{lim_{dow}}, \mathrm{lim_{up}})$, where $\mathrm{lim_{dow}} = \mathrm{ads_{max,exp}} + W\mathrm{ads_{max,exp}}$ and $\mathrm{lim_{up}} = \mathrm{ads_{max,exp}} - W\mathrm{ads_{max,exp}}$, respectively, and W is chosen as low as possible (i.e., 0.1).

The results are shown in Figs. 9–12. Fig. 9 shows the results obtained based only on the approximation of adsorption data applying the DD and HDDM (two types of the Langmuir sites are assumed). It is seen that the HDDM describes

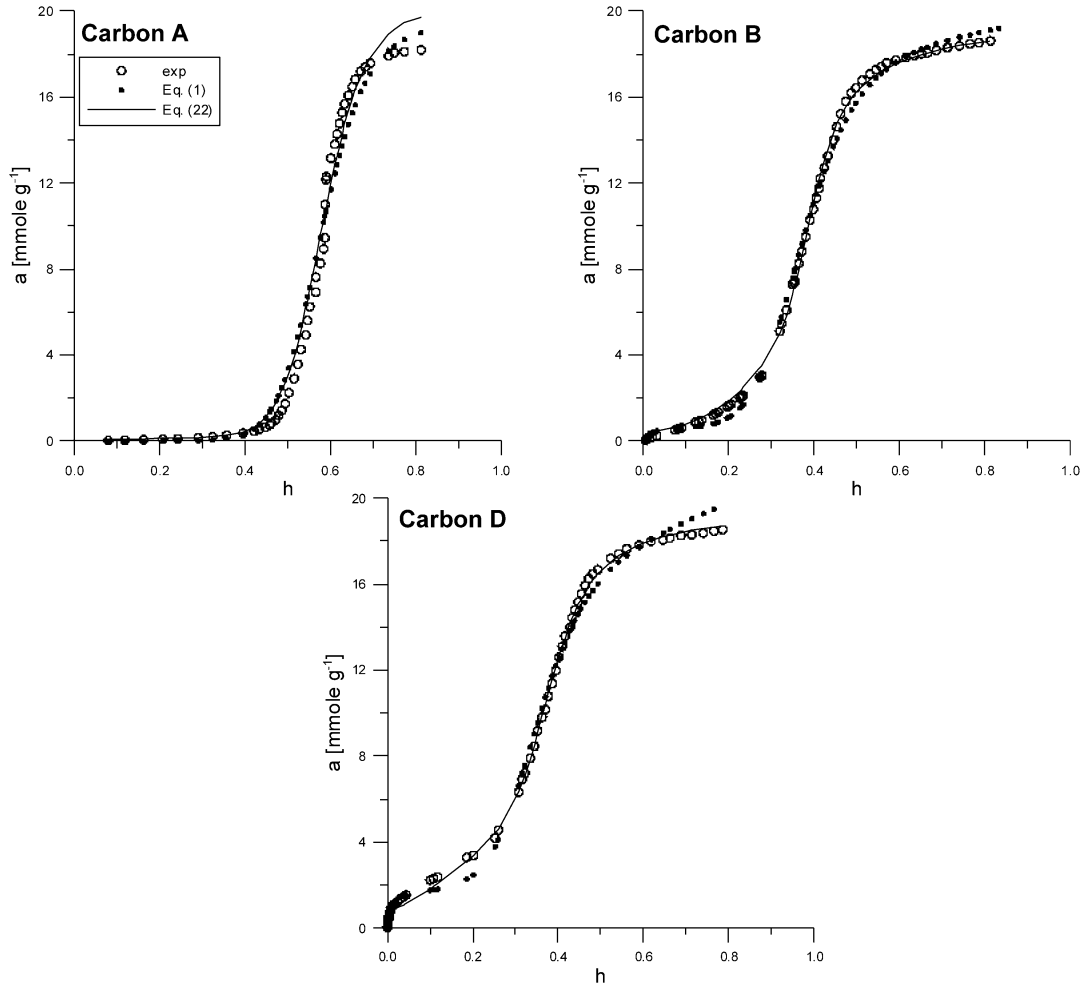

Fig. 9. The fit of the DD model (Eq. (1), closed circles) and HDDM (Eq. (22), two types of the Langmuir sites are assumed; solid line) to the experimental data (open circles) of water adsorption on carbon A (Eq. (1): $DC_{iz} = 0.9829$; Eq. (22): $DC_{iz} = 0.9858$), B (Eq. (1): $DC_{iz} = 0.9970$; Eq. (22): $DC_{iz} = 0.9989$), and D (Eq. (1): $DC_{iz} = 0.9960$; Eq. (22): $DC_{iz} = 0.9993$), respectively. The calculations were performed in the whole range of relative pressures.

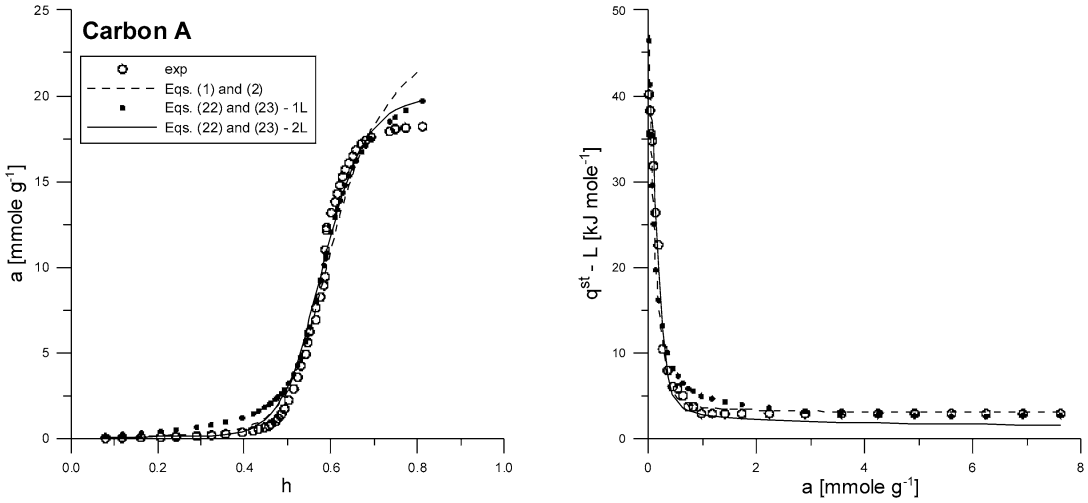

Fig. 10. The fit of the DD model (Eq. (1) with Eq. (2); dashed line) and HDDM (Eq. (22) with Eq. (23); one (1L; closed circles) or two (2L; solid line) types of the Langmuir sites are assumed, respectively) to the experimental data (open circles) of water adsorption on carbon A. The calculations were performed in the whole range of relative pressures. DD: $DC_{Iz} = 0.9700$; $DC_{qst} = 0.9608$; $DC_{Iz\_qst} = 0.9657$. HDDM(1L): $DC_{Iz} = 0.9834$; $DC_{qst} = 0.9467$; $DC_{Iz\_qst} = 0.9702$. HDDM(2L): $DC_{Iz} = 0.9841$; $DC_{qst} = 0.9863$; $DC_{Iz\_qst} = 0.9852$.

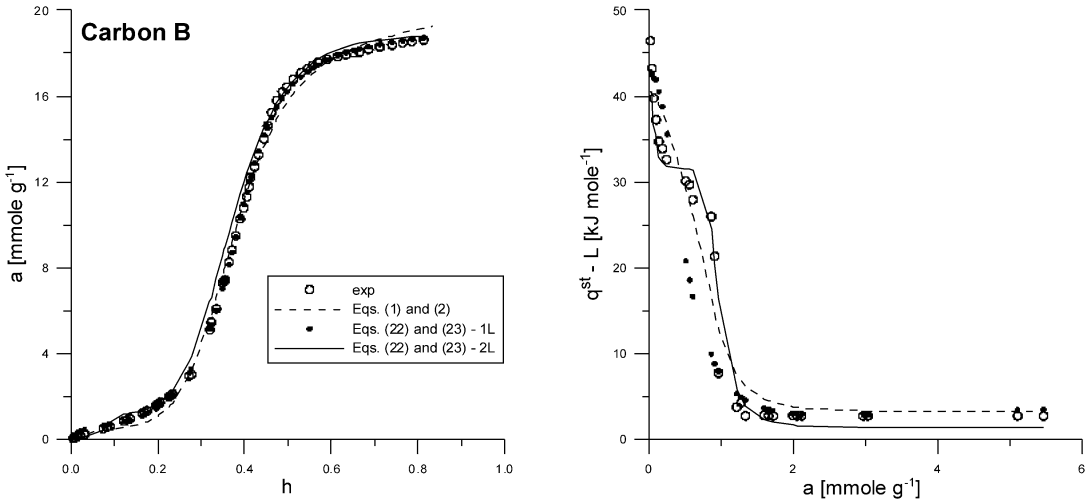

Fig. 11. The fit of the DD model (Eq. (1) with Eq. (2); dashed line) and HDDM (Eq. (22) with Eq. (23); one (1L; closed circles) or two (2L; solid line) types of the Langmuir sites are assumed, respectively) to the experimental data (open circles) of water adsorption on carbon B. The calculations were performed in the whole range of relative pressures. DD: $DC_{Iz} = 0.9967$; $DC_{qst} = 0.9570$; $DC_{Iz\_qst} = 0.9882$. HDDM(1L): $DC_{Iz} = 0.9996$; $DC_{qst} = 0.8992$; $DC_{Iz\_qst} = 0.9934$. HDDM(2L): $DC_{Iz} = 0.9955$; $DC_{qst} = 0.9941$; $DC_{Iz\_qst} = 0.9949$.

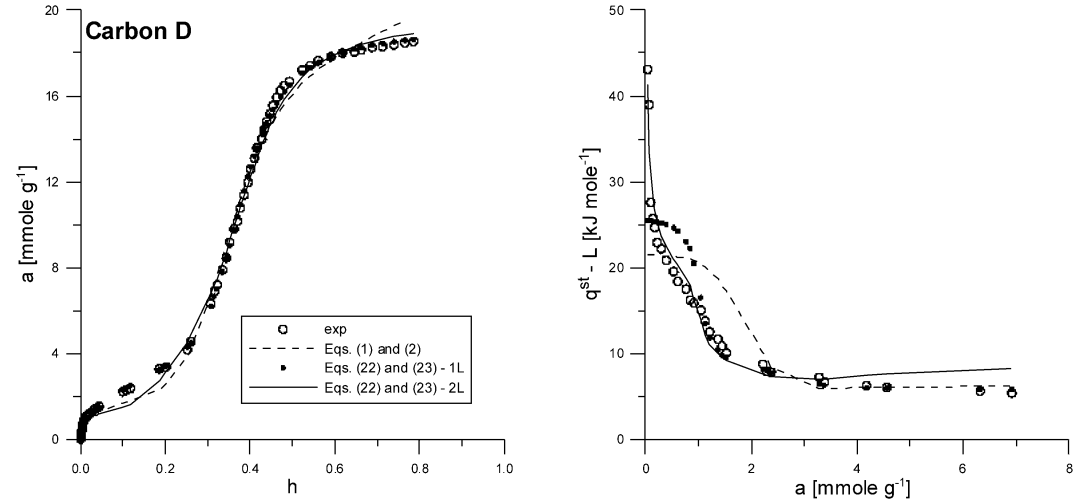

Fig. 12. The fit of the DD model (Eq. (1) with Eq. (2); dashed line) and HDDM (Eq. (22) with Eq. (23); one (1L; closed circles) or two (2L; solid line) types of the Langmuir sites are assumed, respectively) to the experimental data (open circles) of water adsorption on carbon D. The calculations were performed in the whole range of relative pressures. DD: $DC_{Iz} = 0.9950$; $DC_{qst} = 0.5352$; $DC_{Iz\_qst} = 0.9518$. HDDM(1L): $DC_{Iz} = 0.9996$; $DC_{qst} = 0.7318$; $DC_{Iz\_qst} = 0.9902$. HDDM(2L): $DC_{Iz} = 0.9965$; $DC_{qst} = 0.9552$; $DC_{Iz\_qst} = 0.9874$.

the data better, however it contains more best-fit parameters. A more interesting comparison between the DD and the HDDM models (one or two types of Langmuir sites are assumed) is observed during the analysis of the results of the simultaneous fitting of the adsorption and related enthalpy data (Figs. 10–12). The fit of adsorption isotherms is similar for all three models; however, the DD model predicts too large adsorption around saturation. On the contrary, the satisfactory fit between theoretical and experimental adsorption enthalpy plots occurs only if the heterogeneity of adsorption sites is taken into account (Figs. 11 and 12). Considering this heterogeneity leads to the complication of the model, however it seems to reflect the real nature of the process of water adsorption on carbons.

7. Conclusions

Presented new model of water adsorption on carbons seems to be the first one describing adsorption and related enthalpy data in the whole relative pressure range. It is shown that for adsorbents possessing different types of surface centers the modification of the original approach proposed by Do and Do leads to remarkable improvement of the fit between theoretical and measured experimentally isotherms and calorimetric enthalpy data.

Moreover, simulated water adsorption isotherms and related enthalpy plots cover all types of the curves measured experimentally by different authors [3,4,6,7,9,10,17–20,28–37].

Presented results confirm that for the verification of a new adsorption model, and proposed mechanism of adsorption, not only the goodness of the fit between theoretical and experimental isotherms should be studied. Since the adsorption isotherm is the combination of the enthalpy and entropy effects, the goodness of the fit between theoretical and calorimetric data is an additional criterion confirming the validity of the model.

Acknowledgments

P.A.G. gratefully acknowledges the financial support from KBN Grant 4T09A 077 24. A.P.T. gratefully acknowledges the financial support from KBN Grant 3 T09A 065 26.

References

[1] D. Mowla, D.D. Do, K. Kaneko, Chem. Phys. Carbon 27 (2003) 229.
[2] J.K. Brennan, T.J. Bandosz, K.T. Thomson, K.E. Gubbins, Colloids Surf. A 187–188 (2001) 539.
[3] R.Sh. Vartapetyan, A.M. Voloshchuk, Chem. Rev. 64 (1995) 985.
[4] P.A. Gauden, A.P. Terzyk, The Theory of Adsorption of Gasses and Vapours in Micropores of Carbonaceous Materials, WIChiR, Warsaw, 2002 (in Polish).
[5] J. Zawadzki, Chem. Phys. Carbon 21 (1989) 147.
[6] A.P. Terzyk, P.A. Gauden, G. Rychlicki, Colloids Surf. A 148 (1999) 271.
[7] A.P. Terzyk, G. Rychlicki, P.A. Gauden, Colloids Surf. A 179 (2001) 39.
[8] R.P. Wesołowski, P.A. Gauden, A.P. Terzyk, S. Furmaniak, Carbon 53 (2004) 42.
[9] P.A. Gauden, J. Colloid Interface Sci. 282 (2005) 249.
[10] S. Furmaniak, P.A. Gauden, A.P. Terzyk, R.P. Wesołowski, G. Rychlicki, submitted for publication.
[11] T. Ohba, H. Kanoh, K. Kaneko, J. Am. Chem. Soc. 126 (2004) 1560.
[12] K. Kaneko, Y. Hanzawa, T. Iiyama, T. Kanda, T. Suzuki, Adsorption 5 (1999) 7.
[13] D.D. Do, H.D. Do, Carbon 38 (2000) 767.
[14] M. Neitsch, W. Heschel, M. Suckov, Carbon 39 (2001) 1437.
[15] L. Cossarutto, T. Zimny, J. Kaczmarczyk, J. Siemieniewska, J. Bimer, J.V. Weber, Carbon 39 (2001) 2339.
[16] C. Vagner, G. Finqueneisel, T. Zimny, J.V. Weber, Fuel Proc. Technol. 77–78 (2002) 409.
[17] M.M. Dubinin, Izv. AN SSSR 1 (1991) 9 (in Russian).
[18] R.S. Vartapetyan, A.M. Voloshchuk, M.M. Dubinin, T.S. Yakubov, Izv. AN SSSR 9 (1987) 1934 (in Russian).
[19] G. Rychlicki, Role of Carbon Surface Chemism in Adsorption and Catalytic Processes, UMK, Toruń, 1985 (in Polish).
[20] G. Rychlicki, Polish J. Chem. 63 (1989) 255.
[21] M. Jorge, C. Schumacher, N.A. Seaton, Langmuir 18 (2002) 9296.
[22] H. Kitano, K. Ichikawa, M. Ide, M. Fukuda, W. Mizuno, Langmuir 17 (2001) 1889.
[23] D. Suarez, J.A. Menendez, E. Fuente, M.A. Montes-Moran, Langmuir 15 (1999) 3897.
[24] M. Jaroniec, R. Madey, Physical Adsorption on Heterogeneous Solids, Elsevier, Amsterdam, 1988.
[25] R. Storn, K. Price, in: Proceedings of 1996 IEEE International Conference on Evolutionary Computation (ICEC '96), Nagoya University, 1996, p. 842.
[26] R. Storn, K. Price, J. Global Optim. 11 (1997) 341.
[27] A.P. Terzyk, J. Chatłas, P.A. Gauden, G. Rychlicki, P. Kowalczyk, J. Colloid Interface Sci. 266 (2003) 473.
[28] R.Sh. Vartapetyan, A.M. Voloshchuk, A.A. Isirikyan, N.S. Olyakov, Yu.I. Tarasevich, Colloids Surf. A 101 (1995) 227.
[29] N.N. Avgul, O.M. Dzigit, A.V. Kiselev, K.D. Sherbakov, Izv. AN SSSR 2 (1953) 105 (in Russian).
[30] M.M. Dubinin, E.D. Zaverina, V.V. Serpinsky, Trans. Faraday Soc. 1760 (1955).
[31] M.M. Dubinin, A.A. Isrikikyan, Izv. AN SSSR 10 (1989) 2183 (in Russian).
[32] K. Miura, T. Morimoto, Langmuir 4 (1988) 1283.
[33] Philips, D. Kelly, L. Radovic, F. Xie, J. Phys. Chem. B 104 (2000) 8170.
[34] H. Naono, M. Hakuman, M. Shimoda, K. Nakai, S. Kondo, J. Colloid Interface Sci. 182 (1996) 230.
[35] M.M. Dubinin, Izv. AN SSSR 1 (1981) 1 (in Russian).
[36] H. Naono, M. Shimoda, N. Morita, M. Hakuman, K. Nakai, S. Kondo, Langmuir 13 (1997) 1297.
[37] A.P. Terzyk, G. Rychlicki, M. Ćwiertnia, P.A. Gauden, P. Kowalczyk, submitted for publication.